ACS OMEGA

http://pubs.acs.org/journal/acsodf

Article

Study on a Natural Silk Cocoon Membrane-Based Versatile and Stable Immunosensing Platform via Directional Immunoaffinity Recognition

Hongmei Wang,[#] Shengbao Duan,[#] Yezhou Chen, Huan Liu, Jingjing Tian, Feiran Wu, Ziqian Du, Longhai Tang, Yong Li, and Shaohua Ding*

Cite This: *ACS Omega* 2022, 7, 35297−35304

Read Online

ACCESS | Metrics & More | Article Recommendations | Supporting Information

ABSTRACT: The development of immunosensing assays for in vitro diagnostics has attracted great attention in recent years. Various substrate materials and immobilization methods of biomolecules were exploited for immunosensors, but their bioactivity and longevity have been facing serious challenges. To address this limitation, we investigated a natural silk cocoon membrane as immunosensing substrate material. By using its intrinsic properties, the target biomolecules were immobilized on the membrane through directional immunoaffinity recognition. The silk cocoon membrane-based immunosensor showed great potential for both qualitative and quantitative immunoassays, through naked-eye observation or analyzing the change in red color intensity, respectively. The immunosensor exhibited significant detection capability for anti-D (titer 1:1024) sensitized red blood cells. The colorimetric responses of concentrations ranged from 1 μg/mL to 1 ng/mL, and the detection limit for anti-D was 3.4 ng/mL. The immunosensor also showed excellent stability for the immobilized antibodies when stored at 4 and 25 °C; the bioactivity remained unchanged or slightly declined within 40 weeks. Even at 37 °C, the bioactivity began to decline after 12 weeks. This current work highlights the potential of using the natural silk cocoon membrane as a substrate for a versatile and thermally stable immunosensing platform for application in immunoassays.

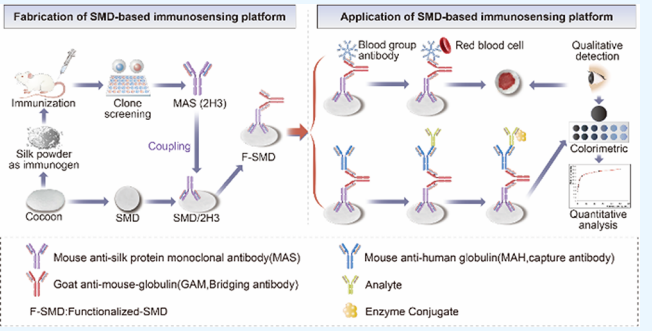

1. INTRODUCTION

The development of immunosensing assays for in vitro diagnostics has witnessed significant and tremendous progress in the past few decades.[1−3] It is known that a critical requirement of diagnostic devices including immunosensors is the longevity of their bioactivity. The choice of substrate material and the attachment method of a biorecognition molecule (antibody or antigen) on the substrate material are two key factors for the longevity of immunosensors. Various substrate materials, such as paper, nanomaterials, metals, and optical fibers, are widely used for immunosensing assays.[4] Especially, paper-based biosensors have been proposed as alternative platforms, because of their availability, inexpensiveness, and ease in being functionalized.[5] However, a biorecognition molecule anchored to the surface of a paper or other substrates with oriented immobilization and natural conformation to ensure its biological activity and functionality remains one of the major challenges in the development and application of a robust and sensitive immunosensor.[6,7] The most common methods of immobilization of biomolecules are direct passive physical adsorption and crosslinker-mediated chemical reactions. The main drawback of the physical adsorption is random orientation, which may affect the binding efficiency, and chemical linker-based immobilization is also not site-specific and may deteriorate the activity of biorecognition molecules due to structural deformation.[8−10] Therefore, continuous efforts have been made to develop a facile and mild method of oriented immobilization of biorecognition molecules and find new substrate materials, to improve the binding efficiency and stability of the immunosensor.[6,7,11,12]

Recently, silk from *Bombyx mori*, which is mainly composed of unique protein biopolymers fibroin and sericin with bioactivity, has been widely used as a biofunctional substrate material due to its good mechanical stability and elasticity, good biocompatibility, biodegradability, and immunogenicity.[13−15] Silk can be regenerated and used to fabricate different substrates for various applications of biosensors.[16−19] Furthermore, silk possesses the ability to stabilize biomolecules.

Received: July 28, 2022
Accepted: September 9, 2022
Published: September 21, 2022

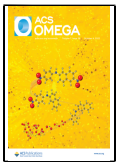

Scheme 1. Schematic Representation of SMD-Based Immunosensing Platform Fabrication and Application

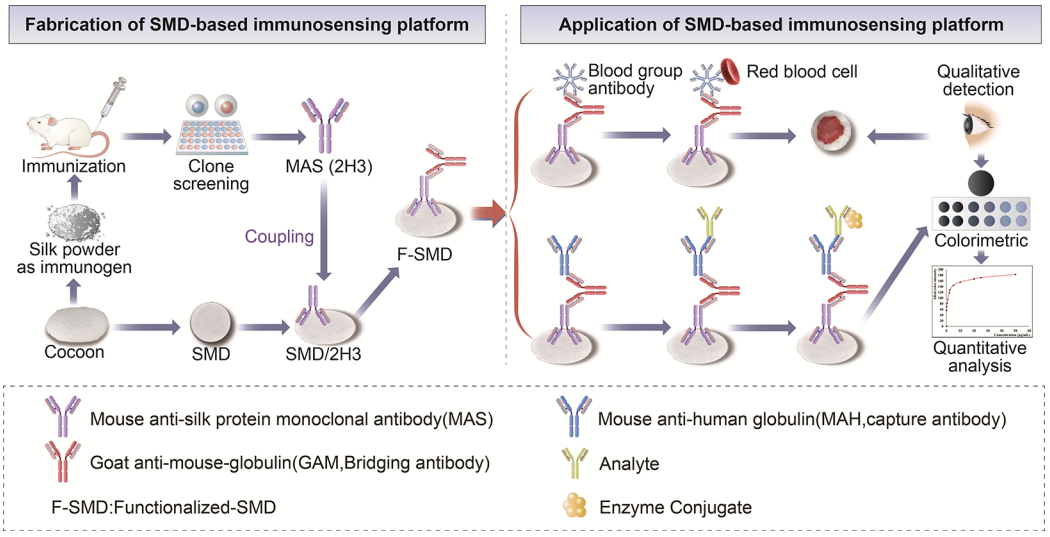

Some researchers consider that the mechanism of stabilization is the higher crystallinity of the β-form structure in the regenerated silk fibroin films, which enhance the stabilization during storage, and others think that silk protein could form a protective barrier by increasing protein−protein interactions and reducing compound or protein mobility to promote protein stability.[20−22] The stabilization effects of silk have been demonstrated in blood components, enzymes, virus, monoclonal antibodies (mAbs), vaccines, antibiotics, DNA, RNA, etc.[23−29]

This paper studied the natural silk cocoon membrane disc (SMD) as a new immunosensing substrate material by using its intrinsic properties, including natural biomembrane structure, composition of fibrous protein biopolymer, and natural stable performance. A specific mouse mAb directed against the silk proteins was used to activate the SMD by site-specific binding. The bridging and capture of antibodies were sequentially bound to the SMD via orderly immunoaffinity recognition, but not through physisorption or chemical modifications. The SMD-based immunosensing platform can be used for both qualitative and quantitative immunoassays (Scheme 1) and provides a general immunosensing substrate and effective immobilization of proteins. SMD-based immunosensors have been successfully applied to the straightforward qualitative detection of blood grouping antigens of RBCs in our previous study.[19] This study aimed to further evaluate the quantitative performance and thermal stability of the SMD-based immunosensing platform.

2. MATERIALS AND METHODS

2.1. SMD, mAbs, and Other Reagents. The silk cocoons from *B. mori* used in this study were purchased from a local market and treated before use. Briefly, the pupae were discarded after cutting open the cocoons. Wax and other impurities were removed by washing with hot water. Then, the cocoons were punched into round discs (8 mm in diameter) using a hole puncher. Discs with a thickness of 0.2 mm ± 0.03 mm were used in further experiments. Then, the SMDs were immersed in PBST and incubated in a water bath at 50 °C for 4 h to improve their permeability. Finally, the discs were washed twice with PBS and stored at 4 °C for later use. The mAb against the silk cocoon (clone 2H3) was prepared in-house. Blood typing antibodies IgG anti-D (2 mg/mL, with a titer of 1:256, clone MS-26), anti-A IgM antibodies (clone BIRMA-1), anti-B IgM antibodies (clone LB-2), and anti-D IgM antibodies (clone RUM-1) were obtained from Millipore, USA. Goat anti-mouse globulin (GAM-IgG), mouse anti-human IgG (MAH-IgG), horseradish peroxidase (HRP)-labeled GAM-IgG, HRP-labeled rabbit anti-goat IgG (RAG-IgG), HRP-labeled rabbit anti-human IgG (RAH-IgG), FITC-labeled GAM-IgG, FITC-labeled RAG-IgG, and precipitate 3,3′,5,5′-tetramethylbenzidine (TMB) substrate were purchased from Sigma-Aldrich, USA. All analytical-grade chemical reagents were purchased from Sinopharm Chemical Reagent Co., Ltd. (China). PBS (1×, pH 7.2) and PBST (1× PBS with 0.05% v/v Tween-20) were prepared in-house. Whole blood samples from adult volunteers were provided by Suzhou Blood Centre. The blood samples were kept at 4 °C and were used within 1 week.

2.2. Fabrication and Characterization of the SMD-Based Immunosensing Platform. The pretreated SMDs were first immersed in a solution of 10 μg/mL 2H3 in PBS at 4 °C overnight. Afterward, the SMDs were washed twice with PBS. HRP-labeled GAM-IgG was used to confirm the binding of 2H3 with colorimetric assays. GAM-IgG-FITC was used as a detection antibody to observe the immobilization and distribution of 2H3 on the SMDs using a confocal laser scanning microscope (TCS Leica SP2, Wetzlar, Germany). The activated SMDs/2H3 were further soaked in 10 μg/mL GAM-IgG solution at 4 °C overnight to form the functionalized SMD (F-SMD). HRP-labeled RAG-IgG and RAG-IgG-FITC were used as detection antibodies to confirm the binding of GAM-IgG to SMDs/2H3, as well as that of 2H3 to the SMDs, also by using colorimetric ELISA and confocal laser scanning microscopy.

Furthermore, the surface morphology and microstructural changes of the SMDs associated with the sequential binding of 2H3 and GAM-IgG antibodies were directly evaluated by atomic force microscopy (AFM) at the nanoscale level. All AFM measurements were performed on a scanning probe microscope (Bruker Multimode 8) using the ScanAsyst mode with a nominal force constant of 0.4 N/m. The tip (Bruker, ScanAsyst-AIR) has a 10° half-cone angle, a 10 nm radius, and a resonance frequency of 50−90 kHz. In the three different

https://doi.org/10.1021/acsomega.2c04777
ACS Omega 2022, 7, 35297−35304

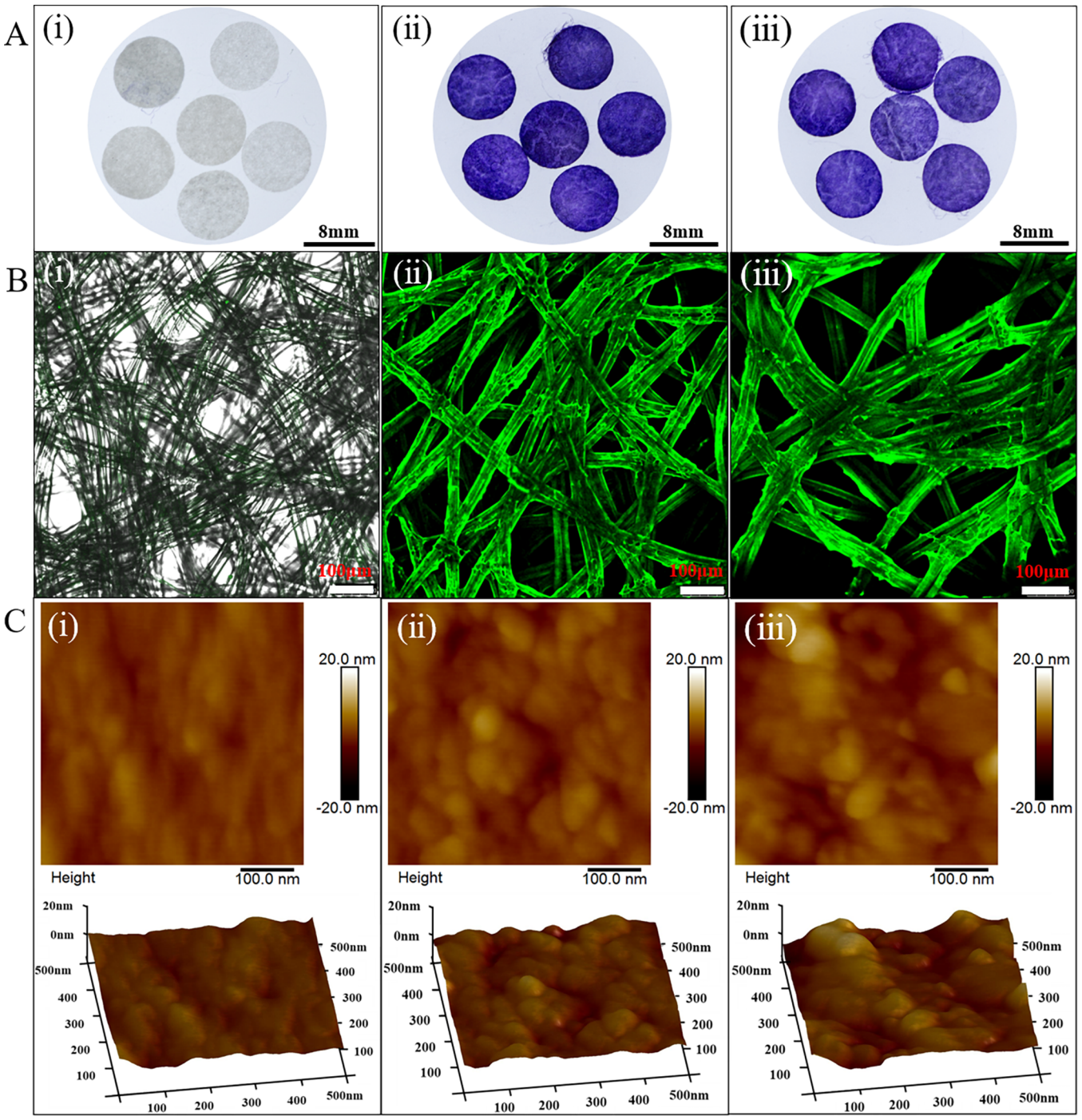

Figure 1. Characterization of the stepwise fabrication process of the SMD-based immunosensing platform. (A) Colorimetric ELISA assays to confirm the binding of 2H3 and GAM-IgG on the SMD; (B) confocal laser scanning microscopy images to confirm the binding of 2H3 and GAM-IgG on the SMD; and (C) AFM images to confirm the binding of 2H3 and GAM-IgG on the SMD. (i) Naked SMDs as the blank control, (ii) SMD/2H3, and (iii) SMD/2H3/GAM-IgG.

means of detection to confirm the immobilization and distribution of 2H3 and GAM-IgG, the SMDs without binding any antibody (naked SMDs) were taken as blank control.

The proper binding amount of 2H3 and the bridging antibody was optimized as follows. The treated SMDs were reacted with different concentrations of 2H3 in the range of 19 ng/mL to 20 μg/mL, with 100 μL antibody per disc. HRP-labeled GAM-IgG was used as a detection antibody to confirm the optimal binding of 2H3 with colorimetric assays. Then, the SMDs/2H3 with an optimal 2H3 concentration were soaked in GAM-IgG at different concentrations in the range of 9 ng/mL to 10 μg/mL and 100 μL/disc at 4 °C overnight. HRP-labeled RAG-IgG was used as a detection antibody to confirm the optimum binding amount of GAM-IgG with colorimetric assays as well. The images of colorimetric SMDs in different concentrations were captured using a digital camera (Praktica, LM20-Z35S), and quantitative analysis was performed using digital image colorimetry (DIC). The RGB (red, green, and blue) color intensity was analyzed using ImageJ (NIH) software. The highest color intensity change was observed on

https://doi.org/10.1021/acsomega.2c04777
ACS Omega 2022, 7, 35297−35304

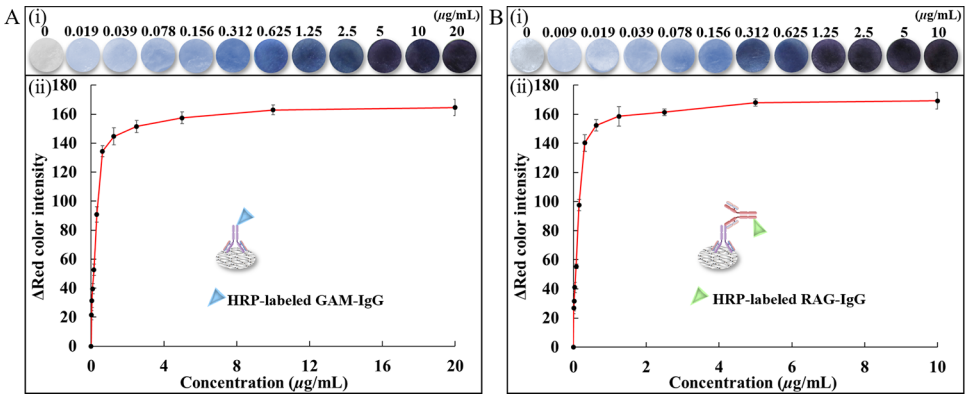

Figure 2. Determination of the optimal binding concentration of antibodies using colorimetric ELISA. (A) SMD/2H3 and (B) SMD/2H3/GAM-IgG. (i) Digital images of the colorimetric ELISA responses. (ii) Quantitative analysis of the ΔRed color intensity of the different binding concentrations with linear regression.

the red channel in this study. Therefore, the change in the red (ΔRed) color intensity was used to quantitatively determine the analytical performance of the immunosensing system.

2.3. Analytical Performance of the SMD-Based Immunosensing Platform. To analyze the performance of the SMD-based immunosensing platform, MAH-IgG as a capture antibody was immobilized onto the SMD/2H3/GAM-IgG overnight at 4 °C to detect the humanized IgG-type anti-D antibody, against the RhD (rhesus D) antigen, based on the principle of the solid-phase antiglobulin test.[30,31] The reaction of anti-D with the SMD/2H3/GAM-IgG/MAH-IgG was detected by using two different color-rendering methods. At first, two-fold serial dilutions of IgG anti-D from 1:1 to 1:1024 were used to sensitize the type O RhD (+) RBCs. The washed RBCs were diluted to 5% with normal saline and mixed at equal volumes with diluted anti-D in a separate tube. The mixture was incubated at 37 °C for 30 min. IgG-type anti-D-sensitized RBCs were washed with normal saline four times and resuspended with normal saline to either 50% for the SMD immunosensor or 5% for the tube antiglobulin test. Then, 5 μL/disc of 50% anti-D sensitized RBCs was added to the SMD/2H3/GAM-IgG/MAH-IgG. Subsequently, 200 μL of PBS was applied to each SMD to elute the unbound blood cells. Unsensitized RBCs were used as the negative control. The adsorption of sensitized and unsensitized RBCs on the SMD/2H3/GAM-IgG/MAH-IgG was observed by the naked eye. At the same time, the tube antiglobulin test was also used for comparison. One hundred microliters of MAH-IgG was added to each tube, which included 100 μL of 5% sensitized RBCs, and it was centrifuged at 200 g for 1 min. The agglutination of RBCs with different anti-D dilutions was observed.

To further analyze the quantitative performance of the SMD-based immunosensing platform, the SMD/2H3/GAM-IgG/MAH-IgG was incubated at 37 °C for 30 min with anti-D, which was diluted from 1 μg/mL to 1 ng/mL and 100 μL/disc, respectively. After washing, 100 μL/disc of HRP-labeled RAH-IgG was added, and the discs were incubated at 37 °C for 30 min. After washing, the TMB substrate was added for chromogenic reaction (100 μL/disc), and the discs were incubated at 37 °C for 10 min. The reaction was stopped by washing the discs three times with pure water. The results were captured with a digital camera and quantitatively analyzed based on DIC.

2.4. Thermal Stability of the SMD-Based Immunosensing Platform. The long-term thermal stability of the SMD-based immunosensing platform was studied at different storage conditions by testing the validity of anti-D on the immunosensors at different time intervals. Air-dried SMD/2H3/GAM-IgG/MAH-IgG were stored at 4, 25, and 37 °C (accelerated stability test) for 40 weeks. At selected time intervals, the activity of the SMD-based immunosensors was determined by detecting anti-D at a concentration of 1 μg/mL by colorimetric ELISA and quantitatively analyzed using DIC.

Additionally, we investigated the long-term stability of the SMD-based immunosensing platform, coupled with blood-type antibodies (anti-A, -B, and -D) at 4, 25, and 37 °C for 20 weeks. At selected time intervals, the stability of the SMD-based immunosensor with immobilized blood group antibodies was determined using RBCs. The application of the SMD-based immunosensor to RBC antigen typing and blood group antibody coupling and blood group antigen detection procedures were described in detail in our previous study.[19]

3. RESULTS AND DISCUSSION

3.1. Characterization and Optimization of the SMD-Based Immunosensing Platform. Instead of using complex surface chemistry activation methods, the SMD was activated and functionalized via a specific mAb and bridging antibody by immunoaffinity recognition. The stepwise construction of the SMD-based immunosensing platform was characterized by colorimetric ELISA, fluorescence microscopy, and AFM, respectively. The HRP-labeled GAM IgG and HRP-labeled RAG-IgG secondary antibodies were used in colorimetric ELISA to validate the binding of specific antibody 2H3 and bridging antibody GAM-IgG. After adding the TMB, the activated SMDs showed a dark-purple color (Figure 1A(ii–iii)), while the control naked SMDs only showed an original white color due to being without 2H3 binding (Figure 1A(i)). An FITC-labeled GAM IgG and an FITC-labeled RAG IgG were used to demonstrate the efficient attachment and homogeneous distribution of the antibodies on the SMDs, which were analyzed by fluorescence microscopy. Upon the attachment of 2H3 and GAM-IgG, the activated SMDs showed a strong fluorescent signal on the silk fibers (Figure 1B(ii–iii)). The image of the control sample shows a basal level of fluorescence in the native SMD (Figure 1B(i)), which could be attributed to the inherent autofluorescence of natural silk.[32] The SMD nanoscale morphological and structural changes

https://doi.org/10.1021/acsomega.2c04777
ACS Omega 2022, 7, 35297−35304

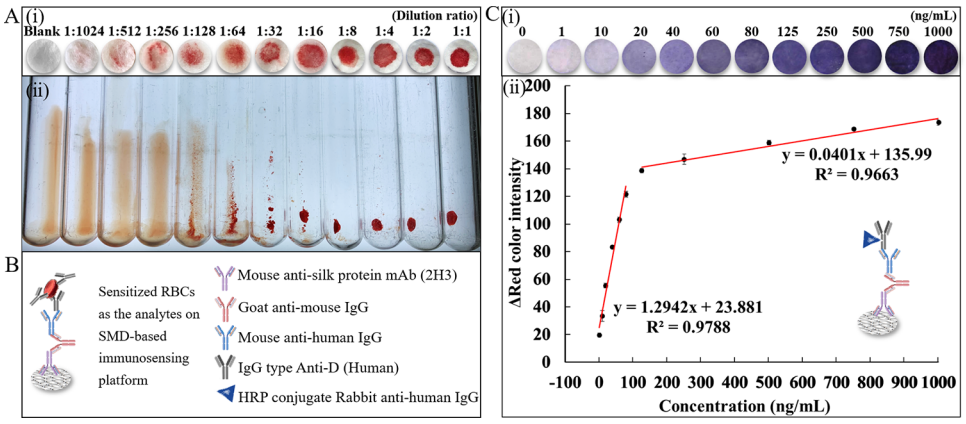

Figure 3. Analytical performance of the SMD immunosensor for the detection of IgG anti-D. (A) Detection of anti-D with the SMD-based immunosensing platform and tube test. (i) Different dilutions of anti-D sensitization of RBCs as the analytes on the SMD-based immunosensing platform; (ii) dilutions of anti-D determined by tube test. (B) Detection principle of anti-D sensitization of RBCs on the SMD-based immunosensing platform. (C) The colorimetric responses of different concentrations ranging from 1 μg/mL to 1 ng/mL using the SMD-based immunosensor. (i) Digital images of the colorimetric responses of anti-D; (ii) linear regression equations for detection of anti-D between low- and high-concentration calibration plots.

were recorded by AFM. Since the natural SMD presents a substantial superficial roughness, we focused on a specific fiber considering its height as a baseline (Figure 1C(i)). The surface nano-roughness increased slightly as the antibody binding process occurred (Figure 1C(ii, iii)). These results demonstrated that 2H3 was successfully bound to the SMDs, and the bridging antibody GAM-IgG was efficiently attached to 2H3, forming F-SMDs.

The efficient binding and uniform distribution of antibodies on the SMD were studied at the macroscopic level and nanoscopic level by the three different methods, indicating its potential as the immunosensor substrate. The specific mAb 2H3 directed against the silk proteins was used to activate the SMD by site-specific binding, through taking advantage of the silk membrane being a kind of substrate with biological activity. The bridging antibodies were sequentially bound to the SMD/2H3 also via efficient immunoaffinity recognitions, which fully retained the bioactivity. The immunoaffinity recognition replaced common physisorption or chemical modifications, which may have resulted in antibody leach-out or reduced antibody activity.[7,10] This affinity binding increased the stability of the binding and enhanced the organization and direction of the binding site.[33] Therefore, controlling the orientation of antibodies will lead to improved analyte binding, resulting in higher biosensor sensitivity.[10]

The determination of the optimal binding concentration of antibodies by colorimetric ELISA is shown in Figure 2A(i) and Figure 2B(i). The optimal concentrations occurred when the reaction between antibodies was saturated, and the ΔRed color intensity remained practically constant (Figure 2A(ii) and Figure 2B(ii)). The optimal concentrations of 2H3 and GAM-IgG were 1.25−2.5 and 0.625−1.25 μg/mL, respectively. Therefore, these concentrations were used to construct the immunosensing platform.

3.2. Analytical Performance of the SMD-Based Immunosensing Platform. In this study, the IgG-type anti-D was used to analyze the performance of the SMD-based immunosensing platform, which was similar to the assay for RBC antigen typing by the indirect antiglobulin test based on paper.[31] The detection model-based solid-phase antiglobulin test taking the IgG-type anti-D as the detection object was used to analyze the performance of the SMD-based immunosensing platform. Figure 3A(i) indicates that the SMD-based immunosensor could detect the higher dilution of anti-D-sensitized RBCs at 1:1024, while the tube method detected the dilution of anti-D at 1:256 (Figure 3A(ii)). The colorimetric ELISA results displayed the colorimetric responses of the SMD-based immunosensor in the presence of different concentrations of anti-D between 1 μg/mL and 1 ng/mL (Figure 3C(i)). The change in the blue color of the immunosensor surface clearly showed a rise in ΔRed color intensity with the increase in anti-D concentrations, indicating that the developed SMD-based immunosensor could effectively detect IgG-type anti-D. Based on the colorimetric responses, two calibration plots were obtained. The linear regression equations for anti-D were expressed for low- and high-concentration calibration plots with correlation coefficients of 0.978 and 0.966, respectively (Figure 3C(ii)). The limit of detection (LOD) of anti-D was determined to be 3.4 ng/mL. The LOD was calculated by three standard deviations of the blank (SDB) divided by the slope (m) of the low-concentration calibration curve ($3 \times \mathrm{SDB}/m$).

The color change of the red channel was highly sensitive to the concentration of the target analyte. Compared to the tube test, the SMD-based immunosensor could detect the higher dilution of anti-D sensitized RBCs, and the relatively low LOD of the anti-D antibody was obtained. Owing to the versatility of natural SMD-based immunosensing platforms in terms of target analytes, they showed great potential for both qualitative and quantitative detection of a broad spectrum of analytes. Additionally, the SMD-based immunosensor developed in this work could be easily applied to any target analyte for which monoclonal/polyclonal antibodies are available. Furthermore, SMDs are natural materials with a three-dimensional porous structure.[34,35] Instead of immobilizing proteins onto a two-dimensional solid surface, captured molecules can diffuse into the porous multilayers of the SMDs. The 3D porous structure of SMDs offers high antibody binding capacity due to its high surface area.

3.3. Thermal Stability of the SMD-Based Immunosensing Platform. Biosensors are prone to aging, which can be characterized as a decrease in signal over time, so stability is

https://doi.org/10.1021/acsomega.2c04777
ACS Omega 2022, 7, 35297−35304

essential for developing a practical biosensor. Silk biomaterials are inherently very stable to changes in temperature and moisture. The silk fibroin possesses a unique ability to stabilize immobilized proteins and small molecules due to its proteins' hydrophobic nature and high glass transition temperature.[20,23,24] In this study, the antibodies were sequentially immobilized on the SMDs by affinity interaction between the antigen and antibody. Through colorimetric ELISA, the results confirmed that the captured antibodies (including MAH-IgG and blood typing antibodies) on the SMD maintained their bioactivity in different storage conditions (Figure 4A). Maybe

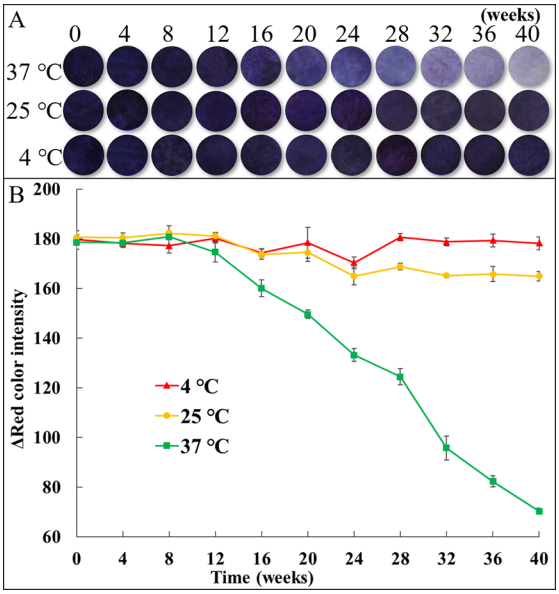

Figure 4. Long-term stability of the SMD-based immunosensing platform stored at different temperatures. (A) Digital images of the colorimetric responses of the SMD/2H3/GAM-IgG/MAH-IgG for the detection of anti-D; (B) quantitative measurement of the ΔRed color intensity of the anti-D detection with linear regression.

due to the protective effect of the silk protein, the bioactivity of MAH-IgG on the SMD probably remained unchanged for 40 weeks when stored at 4 °C, the stability slightly declined within 40 weeks when stored at 25 °C, especially at higher temperatures (37 °C), and the bioactivity began to decline slightly after 12 weeks of storage according to the change in ΔRed color intensity (Figure 4B). Comparing with the stability of 2H3 and 2H3/GAM-IgG coated on microplates without any protective agent (Figure S1), the SMD-based immunosensing platform showed a superior thermal stability, which was able to withstand prolonged high-temperature stress.

Figure 5 shows the thermal stability results of the SMD-based immunosensor with blood typing antibodies (anti-A, anti-B, and anti-D) at 4, 25, and 37. The three groups of antibodies on the SMD-based immunosensor retained a stable activity within 20 weeks under 25 and 4 °C. However, the three groups of antibodies on the SMD-based immunosensor have also begun to lose the ability to agglutinate antigen-positive RBCs after 12 weeks of storage at 37 °C, which was similar to the MAH-IgG detected by colorimetric ELISA. It was superior to the stability of the primary blood typing antibodies, which experienced direct passive physical adsorption and dried on the paper.[36] Formulations unstable at temperatures ≥25 °C are difficult to transport and store,

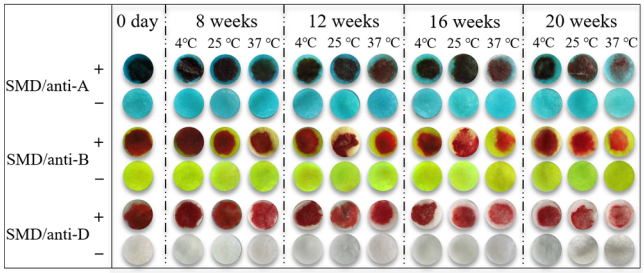

Figure 5. Thermal stability of the SMD-based immunosensor with blood typing antibodies at different storage conditions.

particularly in locations with inadequate refrigeration systems. Since the SMD-based immunosensor developed in this work can be stored at room temperature, without the need of cold-chain equipment, it could be a reasonable solution for such resource-limited settings in the future.

4. CONCLUSIONS

In summary, this study describes investigations into the use of the natural silk cocoon membrane as substrate material for immunosensing due to its thermal stability at different temperatures. The specific mAbs, bridging antibodies, and capture antibodies could sequentially and directionally bind and uniformly distribute on the SMD via immunoaffinity recognitions, to form a versatile and stable immunosensing platform. The developed immunosensor demonstrated great potential for both qualitative and quantitative immunoassay detection. The SMD-based immunosensors show satisfactory stability during long-term ambient storage, which is especially suitable for applications in resource-limited settings. The SMD can be used as a general substrate material to develop novel immunosensing platforms for a wide spectrum of analytes.

■ ASSOCIATED CONTENT

Supporting Information

The Supporting Information is available free of charge at https://pubs.acs.org/doi/10.1021/acsomega.2c04777.

Additional experimental details about the stability of 2H3 and 2H3/GAM-IgG coated on common microplates without any protective agent; the stability of 2H3 and 2H3/GAM-IgG coated on the microplate without any protective agent (PDF)

■ AUTHOR INFORMATION

Corresponding Author

Shaohua Ding − *CAS Key Lab of Bio-Medical Diagnostics, Suzhou Institute of Biomedical Engineering and Technology, Chinese Academy of Sciences, Suzhou, Jiangsu Province 215163, China; Jihua Laboratory, Foshan 528200, China;* orcid.org/0000-0001-7561-9834; Phone: (+086) 512 69588315; Email: dingsh@sibet.ac.cn; Fax: (+086) 512 69588315

Authors

Hongmei Wang − *CAS Key Lab of Bio-Medical Diagnostics, Suzhou Institute of Biomedical Engineering and Technology, Chinese Academy of Sciences, Suzhou, Jiangsu Province 215163, China; Jihua Laboratory, Foshan 528200, China*

Shengbao Duan − *CAS Key Lab of Bio-Medical Diagnostics, Suzhou Institute of Biomedical Engineering and Technology,*

https://doi.org/10.1021/acsomega.2c04777
ACS Omega 2022, 7, 35297−35304

Chinese Academy of Sciences, Suzhou, Jiangsu Province 215163, China; Jihua Laboratory, Foshan 528200, China

Yezhou Chen − *CAS Key Lab of Bio-Medical Diagnostics, Suzhou Institute of Biomedical Engineering and Technology, Chinese Academy of Sciences, Suzhou, Jiangsu Province 215163, China; Jihua Laboratory, Foshan 528200, China*

Huan Liu − *Suzhou Guoke Sibeta Biotechnology Co., Ltd., Suzhou 215163, China*

Jingjing Tian − *CAS Key Lab of Bio-Medical Diagnostics, Suzhou Institute of Biomedical Engineering and Technology, Chinese Academy of Sciences, Suzhou, Jiangsu Province 215163, China*

Feiran Wu − *Jihua Laboratory, Foshan 528200, China*

Ziqian Du − *Jihua Laboratory, Foshan 528200, China*

Longhai Tang − *Suzhou Blood Centre, Suzhou 215163, China*

Yong Li − *CAS Key Lab of Bio-Medical Diagnostics, Suzhou Institute of Biomedical Engineering and Technology, Chinese Academy of Sciences, Suzhou, Jiangsu Province 215163, China; Jihua Laboratory, Foshan 528200, China*

Complete contact information is available at: https://pubs.acs.org/10.1021/acsomega.2c04777

Author Contributions

[#]H.W. and S.Du. contributed equally to this work. The manuscript was written through contributions of all authors. All authors have given approval to the final version of the manuscript.

Notes

The authors declare no competing financial interest.

■ ACKNOWLEDGMENTS

H.W. and S.Du. acknowledge the support from the Research Fund of Jihua Laboratory (Grant X190171TD190) and the Basic Research Pilot Project of Suzhou (Grant SJC2021015). S.Di. acknowledges the financial support from the National Natural Science Foundation of China (Grant 52103135) and the Scientific Research Instrument and Equipment Development Project of the Chinese Academy of Sciences (Grant YJKYYQ20200037).

■ REFERENCES

(1) Balahura, L. R.; Stefan-Van Staden, R. I.; Van Staden, J. F.; Aboul-Enein, H. Y. Advances in immunosensors for clinical applications. *J. Immunoassay Immunochem.* **2019**, *40*, 40−51.

(2) Gopinath, S. C.; Tang, T. H.; Citartan, M.; Chen, Y.; Lakshmipriya, T. Current aspects in immunosensors. *Biosens. Bioelectron.* **2014**, *57*, 292−302.

(3) Justino, C. I. L.; Duarte, A. C.; Rocha-Santos, T. A. P. Immunosensors in Clinical Laboratory Diagnostics. *Adv. Clin. Chem.* **2016**, *73*, 65−108.

(4) Aydin, M.; Aydin, E. B.; Sezginturk, M. K. Advances in immunosensor technology. *Adv. Clin. Chem.* **2021**, *102*, 1−62.

(5) Zhu, G.; Yin, X.; Jin, D.; Zhang, B.; Gu, Y.; An, Y. Paper-based immunosensors: Current trends in the types and applied detection techniques. *TrAC Trend Anal Chem* **2019**, *111*, 100−117.

(6) Li, Z.; Chen, G. Y. Current Conjugation Methods for Immunosensors. *Nanomaterials* **2018**, *8*, 278.

(7) Welch, N. G.; Scoble, J. A.; Muir, B. W.; Pigram, P. J. Orientation and characterization of immobilized antibodies for improved immunoassays (Review). *Biointerphases* **2017**, *12*, No. 02D301.

(8) Nakanishi, K.; Sakiyama, T.; Imamura, K. On the adsorption of proteins on solid surfaces, a common but very complicated phenomenon. *J. Biosci. Bioeng.* **2001**, *91*, 233−244.

(9) Rusmini, F.; Zhong, Z.; Feijen, J. Protein immobilization strategies for protein biochips. *Biomacromolecules* **2007**, *8*, 1775−1789.

(10) Trilling, A. K.; Beekwilder, J.; Zuilhof, H. Antibody orientation on biosensor surfaces: a minireview. *Analyst* **2013**, *138*, 1619−1627.

(11) Lee, Y.; Jeong, J.; Lee, G.; Moon, J. H.; Lee, M. K. Covalent and Oriented Surface Immobilization of Antibody Using Photoactivatable Antibody Fc-Binding Protein Expressed in Escherichia coli. *Anal. Chem.* **2016**, *88*, 9503−9509.

(12) Lou, D.; Ji, L.; Fan, L.; Ji, Y.; Gu, N.; Zhang, Y. Antibody-Oriented Strategy and Mechanism for the Preparation of Fluorescent Nanoprobes for Fast and Sensitive Immunodetection. *Langmuir* **2019**, *35*, 4860−4867.

(13) Wray, L. S.; Hu, X.; Gallego, J.; Georgakoudi, I.; Omenetto, F. G.; Schmidt, D.; Kaplan, D. L. Effect of processing on silk-based biomaterials: Reproducibility and biocompatibility. *J. Biomed. Mater. Res., Part B* **2011**, *99b*, 89−101.

(14) Omenetto, F. G.; Kaplan, D. L. New opportunities for an ancient material. *Science* **2010**, *329*, 528−531.

(15) Huang, W.; Ling, S.; Li, C.; Omenetto, F. G.; Kaplan, D. L. Silkworm silk-based materials and devices generated using bio-nanotechnology. *Chem. Soc. Rev.* **2018**, *47*, 6486−6504.

(16) Li, K.; Li, P.; Fan, Y. The assembly of silk fibroin and graphene-based nanomaterials with enhanced mechanical/conductive properties and their biomedical applications. *J. Mater. Chem. B* **2019**, *7*, 6890−6913.

(17) Leal-Egaña, A.; Scheibel, T. Silk-based materials for biomedical applications. *Biotechnol. Appl. Biochem.* **2010**, *55*, 155−167.

(18) Liu, Y.; Tao, L. Q.; Wang, D. Y.; Zhang, T. Y.; Yang, Y.; Ren, T. L. Flexible, highly sensitive pressure sensor with a wide range based on graphene-silk network structure. *Appl. Phys. Lett.* **2017**, *110*, 123508.

(19) Wang, H.; Duan, S.; Wang, M.; Wei, S.; Chen, Y.; Chen, W.; Li, Y.; Ding, S. Silk cocoon membrane-based immunosensing assay for red blood cell antigen typing. *Sens. Actuators, B* **2020**, *320*, 128376.

(20) Li, A. B.; Kluge, J. A.; Guziewicz, N. A.; Omenetto, F. G.; Kaplan, D. L. Silk-based stabilization of biomacromolecules. *J. Controlled Release* **2015**, *219*, 416−430.

(21) Hou, T. C.; Jeng, S. C. Application of Bombyx mori Silk Fibroin Films for Liquid-Crystal Devices. *ACS Appl. Bio Mater.* **2020**, *3*, 8575−8580.

(22) Pritchard, E. M.; Dennis, P. B.; Omenetto, F.; Naik, R. R.; Kaplan, D. L. Review physical and chemical aspects of stabilization of compounds in silk. *Biopolymers* **2012**, *97*, 479−498.

(23) Guziewicz, N. A.; Massetti, A. J.; Perez-Ramirez, B. J.; Kaplan, D. L. Mechanisms of monoclonal antibody stabilization and release from silk biomaterials. *Biomaterials* **2013**, *34*, 7766−7775.

(24) Kluge, J. A.; Li, A. B.; Kahn, B. T.; Michaud, D. S.; Omenetto, F. G.; Kaplan, D. L. Silk-based blood stabilization for diagnostics. *Proc. Natl. Acad. Sci. U. S. A.* **2016**, *113*, 5892−5897.

(25) Lu, Q.; Wang, X.; Hu, X.; Cebe, P.; Omenetto, F.; Kaplan, D. L. Stabilization and release of enzymes from silk films. *Macromol. Biosci.* **2010**, *10*, 359−368.

(26) Zhang, J.; Pritchard, E.; Hu, X.; Valentin, T.; Panilaitis, B.; Omenetto, F. G.; Kaplan, D. L. Stabilization of vaccines and antibiotics in silk and eliminating the cold chain. *Proc. Natl. Acad. Sci. U. S. A.* **2012**, *109*, 11981−11986.

(27) Sutherland, T. D.; Sriskantha, A.; Church, J. S.; Strive, T.; Trueman, H. E.; Kameda, T. Stabilization of Viruses by Encapsulation in Silk Proteins. *ACS Appl. Mater. Interfaces* **2014**, *6*, 18189−18196.

(28) Liu, Y.; Zheng, Z.; Gong, H.; Liu, M.; Guo, S.; Li, G.; Wang, X.; Kaplan, D. L. DNA preservation in silk. *Biomater Sci-Uk* **2017**, *5*, 1279−1292.

(29) He, J.; Yavuz, B.; Kluge, J. A.; Li, A. B.; Omenetto, F. G.; Kaplan, D. L. Stabilization of RNA Encapsulated in Silk. *ACS Biomater. Sci. Eng.* **2018**, *4*, 1708−1715.

(30) Ching, E. Solid Phase Red Cell Adherence Assay: a tubeless method for pretransfusion testing and other applications in transfusion science. *Transfus. Apher. Sci.* **2012**, *46*, 287−291.
(31) Yeow, N.; McLiesh, H.; Guan, L.; Shen, W.; Garnier, G. Paper-based assay for red blood cell antigen typing by the indirect antiglobulin test. *Anal. Bioanal. Chem.* **2016**, *408*, 5231−5238.
(32) Amirikia, M.; Shariatzadeh, S. M. A.; Jorsaraei, S. G. A.; Mehranjani, M. S. Auto-fluorescence of a silk fibroin-based scaffold and its interference with fluorophores in labeled cells. *Eur. Biophys. J.* **2018**, *47*, 573−581.
(33) Wang, X.; Kaplan, D. L. Functionalization of silk fibroin with NeutrAvidin and biotin. *Macromol. Biosci.* **2011**, *11*, 100−110.
(34) Chen, F.; Porter, D.; Vollrath, F. Silk cocoon (Bombyx mori): multi-layer structure and mechanical properties. *Acta Biomater.* **2012**, *8*, 2620−2627.
(35) Chen, F. J.; Porter, D.; Vollrath, F. Morphology and structure of silkworm cocoons. *Mater. Sci. Eng. C* **2012**, *32*, 772−778.
(36) Guan, L.; Cao, R.; Tian, J.; McLiesh, H.; Garnier, G.; Shen, W. A preliminary study on the stabilization of blood typing antibodies sorbed into paper. *Cellulose* **2014**, *21*, 717−727.

https://doi.org/10.1021/acsomega.2c04777
ACS Omega 2022, 7, 35297−35304